

Forecasting of fog/cloud and precipitation by the Battlescale Forecast Model (BFM)

Teizi Henmi

US Army Research Laboratory

Information Sciences and Technology Directorate

Battlefield Environment Division

White Sands Missile Range, New Mexico 88002-5501

The Battlescale Forecast Model (BFM), which was developed at the US Army Research Laboratory (ARL), is a major part of the US Army Integrated Meteorological System (IMETS) Block II software. The BFM can be used operationally over any part of the world by using meteorological data obtained through the Automated Weather Distribution System (AWDS).

The BFM is capable of making 24 hour weather forecast which includes wind, temperature, and relative humidity, as well as fog/cloud coverage and precipitation rate/amount. In the model, the cloud liquid water content is calculated by using the probability density function (Sommeria and Deardoff, 1977, Mellor, 1977, and Yamada and Mellor, 1979), and the precipitation rate/amount are calculated by the scheme of Sundqvist et al (1989).

The model has been applied to several precipitation cases over different areas, and produced reasonable forecast results.

I. Introduction

The U.S. Army Research Laboratory, Battlefield Environment Directorate (ARL, BED) has developed the Battlescale Forecast Model (BFM) for operational short-range (up to 24 hours) forecasting over areas of 500 km by 500 km or smaller. The BFM can be used operationally over any part of the world by using meteorological data obtained through the U.S. Air Force Automated Weather Distribution System (AWDS), and is a major part of the U.S. Army Integrated Meteorological System (IMETS) Block II software. Meteorological data includes the U.S. Air Force Global Spectral Model (GSM) gridded forecast data, in addition to conventional upper air sounding and surface data.

The BFM is composed of several elements such as (1) terrain elevation data deduction program, (2) three dimensional data analysis programs for initialization and assimilation, (3) prognostic mesoscale model, HOTMAC (Yamada and Bunker, 1989), (4) horizontal and vertical displays of forecasting results, (5) graphical user interfaces for execution of the BFM and for display of different output, (6) input/output archiving system, and (7) map background module to help execution and display.

The objectives of the present paper are to describe how cloud/fog and precipitation are calculated in the BFM, and to show some examples of fog/cloud and precipitation forecast results.

II. Cloud/Fog formation

In most of the mesoscale models (i.e, Gelding, 1990, Pielke et al, 1992, Anthes and Warner, 1978), the critical humidity for cloud formation is saturation over water or ice, which depends on temperature, and all water vapor in excess of water/ice saturation is converted to cloud water/ice.

Furthermore, it is assumed that a computational grid volume is either entirely saturated or entirely unsaturated. Even for a relatively small grid volume such as $(50 \text{ m})^3$, this assumption is sometimes in error because substantial portions of cloud volume may contain unsaturated air near the cloud edge or in the cloud due to mixing and entrainment (Sommeria and Deardorff, 1977).

The present scheme takes into consideration the dependencies of mean cloud fraction and mean liquid (cloud) water content upon humidity statistics, assuming Gaussian quasi-conservative properties. It is assumed that the quasi-conservative variables, liquid water potential temperature (θ_l) and liquid water mixing ratio (Q_l) have the Gaussian joint normal probability distributions within any given volume. This assumption implies that those air parcels existing within any given volume have had complicated past trajectories and have not selectively been subjected to rapid changes in θ_l and Q_l .

The Gaussian joint normal distribution function is given by:

$$G = \frac{1}{2\pi\sigma_{\theta_l}\sigma_{q_w}(1-r^2)^{1/2}} \exp\left[-\frac{1}{(1-r^2)}\left(\frac{\theta_l^2}{2\sigma_{\theta_l}^2} - r\frac{\theta_l q_w}{\sigma_{\theta_l}\sigma_{q_w}} + \frac{q_w^2}{2\sigma_{q_w}^2}\right)\right] \quad (1)$$

where θ_l and q_w are the fluctuations of, respectively, liquid water potential temperature and total water mixing ratio, and

$$\sigma_{\theta_l}^2 = \overline{\theta_l^2} \quad (2)$$

$$\sigma_{q_w}^2 = \overline{q_w^2} \quad (3)$$

$$r = \frac{\overline{\theta_l q_w}}{\sigma_{\theta_l}\sigma_{q_w}} \quad (4)$$

Overbars represent the mean properties of variables. The local condensation is assumed to be

given by

$$Q_l = (Q_w - Q_s)H(Q_w - Q_s) \quad (5)$$

where Q_w is total cloud water content, Q_s is saturation mixing ratio, and $H(x)$ is a Heaviside function, defined as

$$H(x) = 0, \quad x < 0 \quad (6)$$

$$1, \quad x > 0$$

Let us define the following parameters:

$$a = (1 + Q_{sl,T} \frac{L_v}{c_p})^{-1} \quad (7)$$

$$b = a \frac{\langle T \rangle}{\langle \theta \rangle} Q_{sl,T} \quad (8)$$

$$\Delta Q = Q_w - Q_{sl} \quad (9)$$

$$Q_{sl,T} \left(\frac{\partial Q_s}{\partial T} \right)_{T=T_l} = 0.622 \frac{L_v}{R_d} \frac{Q_{sl}}{T_l^2} \quad (10)$$

$$Q_{sl} = 0.622 e_s(T_l) / (P - e_s(T_l)) \quad (11)$$

$$e_s(T_l) = 6.11 \exp \left[\frac{L_v}{R_w} \left(\frac{1}{273} - \frac{1}{T_l} \right) \right] \quad (12)$$

and

$$T_l = (P/P_0)^k \theta_l \quad (13)$$

Here Q_{sl} is the mean saturation mixing ratio of water vapor at T_l ; T_l is the liquid water temperature, $e_s(T_l)$ is the saturation water vapor pressure at T_l , R_w is the gas constant for water vapor, and L_v is the latent heat of condensation.

A function R which indicates a fraction of cloud coverage for a given volume of air is given by (Mellor, 1977):

$$R = \int_{-\infty}^{\infty} \int_{-\infty}^{\infty} H(Q_w - Q_s) G dQ_w d\theta_l = \frac{1}{2} [1 + \text{erf}(Q_l/\sqrt{2})] \quad (14)$$

$$\text{erf}(x) = \frac{2}{\sqrt{\pi}} \int_0^x \exp(-y^2) dy \quad (15)$$

Cloud water mixing ratio Q_i is given by:

$$Q_i = 2\sigma_s \left[RQ_1 + \frac{1}{\sqrt{2\pi}} \exp\left(-\frac{Q_1^2}{2}\right) \right] \quad (16)$$

where

$$Q_1 = a \frac{\Delta Q}{2\sigma_s} \quad (17)$$

$$\sigma_s^2 = \frac{1}{4} (a^2 \overline{q_w^2} - 2ab \overline{q_w \theta_i} + b^2 \overline{\theta_i^2}) \quad (18)$$

Finally, q_c^2 , the variance of the cloud water mixing ratio, is expressed as

$$\frac{\overline{q_c^2}}{4\sigma_s^2} = R \left[1 + \left(Q_1 - 2\frac{Q_i}{2\sigma_s} \right) \right] \cdot \left(Q_1 - \frac{Q_i}{2\sigma_s} \right) \frac{1}{\sqrt{2\pi}} \exp\left[-\frac{Q_1^2}{2}\right] \quad (19)$$

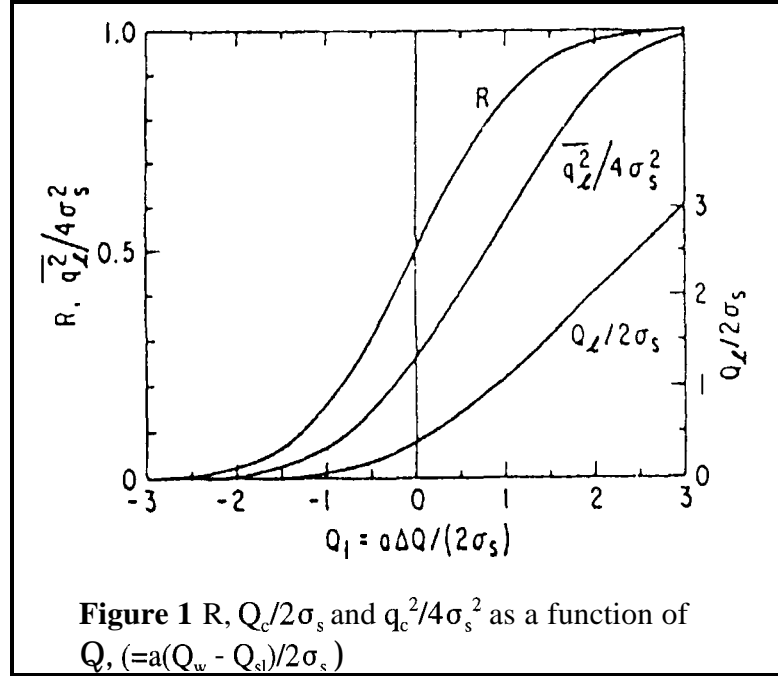
Figure 1 shows R , $Q_c/2\sigma_s$, and $q_c^2/4\sigma_s^2$ as a function of Q_1 obtained according to eqns. (14), (16), and (19), respectively.

As seen from Figure 1, a fraction of cloud coverage R varies gradually with Q_1 and takes non-zero values even if Q_1 is negative. In other words, clouds can exist even if the mixing ratio of water vapor averaged over a grid volume is not saturated. This is realistic because the grid spacing normally used in mesoscale models is larger than the size of small clouds. Therefore, the present cloud model can use a relatively large grid spacing that could save computational time substantially. A statistical cloud model such as the present one avoids the ambiguous condensation criteria often used by coarse grid models; saturation values are lowered arbitrarily to compensate for the amount of cloud that is not resolved by grid.

In the BFM, the total cloud water content, W_{total} , from the ground surface to the top of model atmosphere is calculated and the horizontal distribution of W_{total} is displayed. W_{total} is calculated as:

$$W_{total} = \int_{z_g}^H \rho Q_c dz = \frac{\bar{H} + z_{gmax} - z_g}{\bar{H}} \int_0^{\bar{H}} \rho Q_c dz \quad (20)$$

where p is the air density.



III Precipitation rate

Since micro-physical processes of precipitation formation are not included in the model, the precipitation rate is parameterized as a function of cloud liquid water. The scheme developed by Sundqvist et al (1989) is incorporated in the BFM. The basic assumption is that the denser the cloud the higher the precipitation rate.

The rate of release of precipitation is described by

$$P = C_0 Q_c [1 - \exp(-\frac{Q_c}{R Q_{c,cr}})] \quad (21)$$

Here, $1/C_0$ is regarded as a characteristic time for the conversion of cloud droplets into precipitation particles (raindrops, or snow particles), R is a fraction of cloud coverage described in the previous section, and $Q_{c,cr}$ is a kind of threshold value for cloud water, which Q_c/R must exceed before the release of precipitation can become efficient. The parameter $Q_{c,cr}$ should have

a value typical of individual cloud type, which is invariant to grid resolution.

The rate of precipitation, $P_r(z^*)$, at a z^* -level is given by

$$P_r(z^*) = \int_0^H \rho_a P dz = \left(\frac{\bar{H} + z_{g,\max} - z}{\bar{H}} \right) \bar{\rho}_a P(z^*) \quad (22)$$

Here, H is the depth of model atmosphere, $z_{g,\max}$ is the highest terrain elevation in model domain, z_g is terrain elevation, and ρ_a is the air density.

In order to simulate the coalescence process, Sundqvist et al (1989) introduced an additional parameter F_∞ . This parameter increases with the rate of precipitation and multiplies C_0 and divides $Q_{c,cr}$. The relation is:

$$F_\infty(z^*) = 1 + C_1 Pr(z^*)^{1/2} \quad (23)$$

Similarly, C_0 increases and $Q_{c,cr}$ decreases by a temperature function, F_{BF} , when the temperature is lower than -5 °C in clouds containing a mixture of droplets and ice crystals (Bergeron-Findeisen mechanism). This formulation is:

$$F_{BF} = 1 + C_2 (268.0 - T(z^*))^{1/2} \quad (24)$$

The two modified parameters C_{0F} and $Q_{(c,cr)F}$ become, respectively:

$$C_{0F} = C_0 F_\infty F_{BF} \quad (25)$$

$$Q_{(c,cr)F} = Q_{c,cr} / (F_\infty F_{BF}) \quad (26)$$

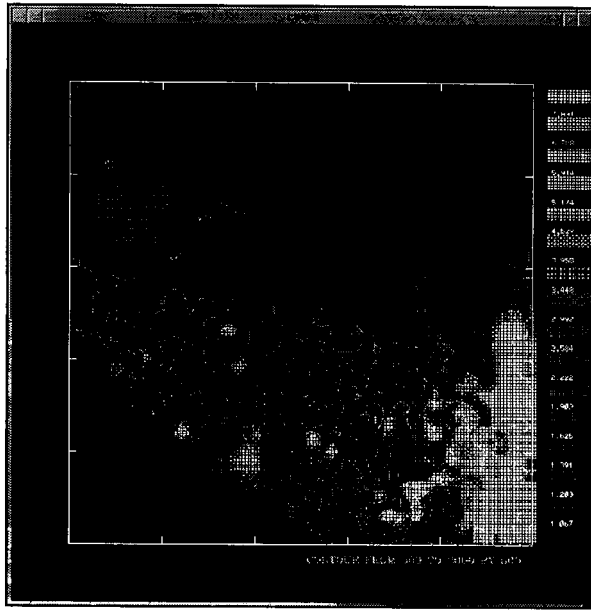
Thus, the precipitation rate at the surface is calculated as:

$$Pr(0) = \left(\frac{\bar{H} + z_{g,\max} - z}{\bar{H}} \right) \frac{1}{\rho_w} \int_0^H \rho_a(z^*) C_{0F} Q_{(c,cr)F}(z^*) [1 - \exp(-(\frac{Q_c(z^*)}{Q_{(c,cr)F}})^2)] dz^* \quad (27)$$

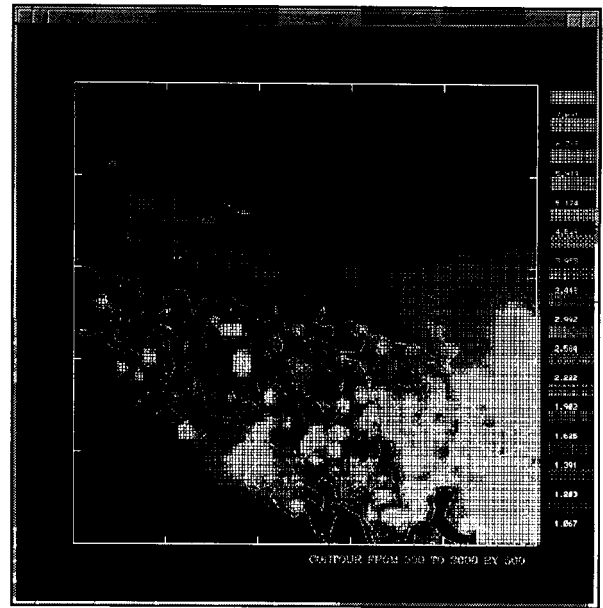
where ρ_w is the density of water. $Pr(0)$ is calculated in the unit of (mm/hr) or (inches/hr).

IV. Examples of fog/low level cloud and precipitation

The BFM was applied to the Bosnia area for the 24 hour period of 12 GMT, December 19 through 12 GMT, December 20, 1995. On December 20, the air traffic over the area was hampered by bad visibility and falling snow. The model simulated cloud formation over the area

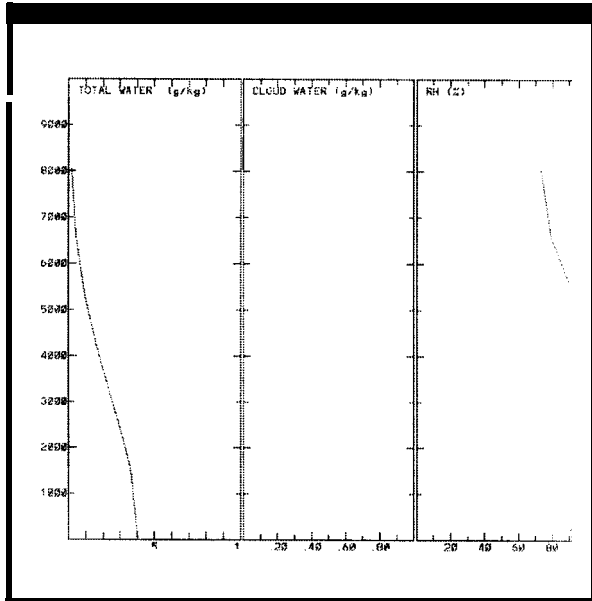


(1)

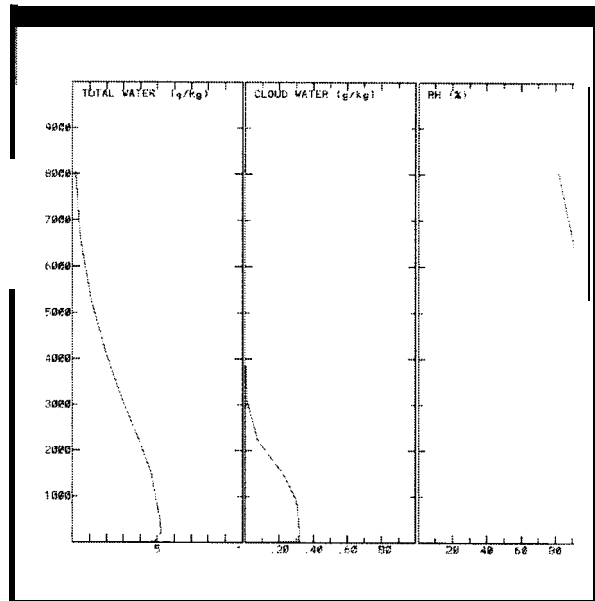


(2)

Figure 2. Cloud cover over Bosnia, (1) at 23 GMT on December 19, 1995, and (2) at 00 GMT on December 20, 1995.



(1)



(2)

Figure 3. Vertical profiles of total water content (g/kg), cloud water content (g/kg), and relative humidity (%), (1) at 00 GMT, and (2) at 01 GMT, December 20, 1995.

at the late evening of December 19, and total cloud coverage over the entire model domain from 01 GMT to 12 GMT of December 20.

Figure 2 (1) and (2) show the cloud coverages at 23 GMT on December 19, and 00 GMT on December 20. The figures show the distribution of the weight of liquid water over a unit area (g/m^2), and the denser the white color, the denser the cloud. The figures may represent the cloud picture taken from far above. As can be seen, the area covered by cloud increased in the one hour, and at 01 GMT on December 20, the entire area was covered by cloud.

Figure 3 (1) and (2) show the vertical profiles of total water content (g/kg), cloud water content (g/kg), and relative humidity (%), at the center point of the model domain. (1) is for 00 GMT, December 20, and (2) is for 01 GMT, December 20. At 01 GMT, the entire area was covered by cloud. In one hour, total water content increased significantly, and cloud water content profiles show significant increase in the lower atmosphere after one hour. The relative humidity has also increased in one hour, and deep layer of atmosphere has become saturated by 01 GMT. From the figures. it can be seen that a very small portion of total water is converted into cloud water.

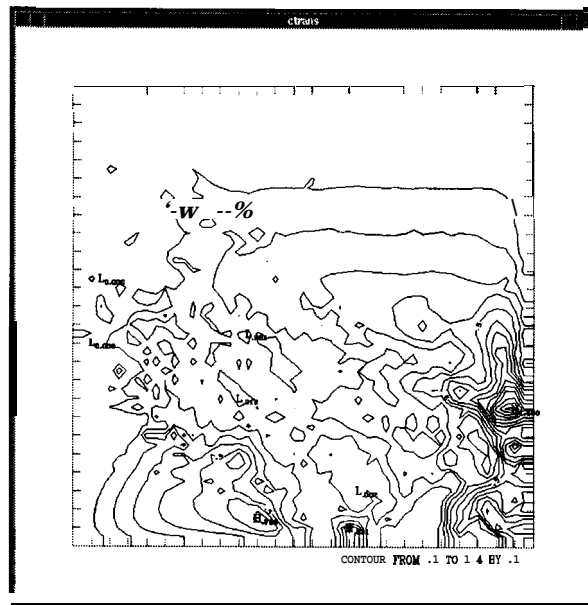


Figure 4. Precipitation rate (mm/hr) distribution over Bosnia, at 01 GMT, December 20, 1995. Maximum rate is $1.4 \text{ mm}/\text{hr}$, and minimum rate is $.1 \text{ mm}/\text{hr}$.

Figure 4 shows the distribution of precipitation rate (mm/hour) at 01 GMT on December 20. The precipitation rate was calculated by the equation 27. The figure shows the precipitation rate varied from 0.1 to $1.4 \text{ mm}/\text{hour}$ over the area. There was no precipitation over the model domain at 00 GMT.

It should be emphasized that fog/cloud and precipitation schemes in the model have yet to be **thoroughly** evaluated, and the results shown should be regarded as preliminary. Further study will be required.

V. Concluding Remarks

The forecasting period of the BFM has been extended to 24 hours, and recently the forecast schemes for fog/cloud as well as non convective precipitation has been added. Other IMETS Block II software such as the Atmospheric Sounding Program (ASP) and the Integrated Weather Effects Decision Aids (IWEDA) utilize the BFM output file to calculate the values of their parameters. ASP generates products such as probability of thunderstorm occurrence, icing, visibility, turbulence, etc.

The BFM is numerically stable, and, as long as reasonable input data are used, the BFM produces numerically reasonable output. Currently, on the IMETS BLOCK II computer (SUN SPARC 20, 75 Mega Hertz, 256 Mega Bytes RAM single processor), the BFM requires about two hours of computing time for the 24 hour forecast duration, using the model configuration of 51 x 51 x 16 grid points and 10 km grid spacing.

The evaluation of the BFM forecasting capability is currently ongoing, and the results will be published in the near future. Forecasting capabilities of wind, temperature and relative humidity, as well as cloud coverage and precipitation amount distribution will be evaluated by comparing the model output and observed data.

The presently-known limitation of the BFM are the following:

- i) Hydrostatic and Boussinesq approximations. Extremely large changes in the large-scale temperature field advected into the BFM grid (via time-dependent boundary values resulting from the GSM) over 24 hours could possibly reduce the validity of the Boussinesq approximation, based on the BFM definition of basic state for θ_v .
- ii) No cloud microphysics.
- iii) No convective cloud parameterization, thus no ability to handle features generated by convective systems, such as meso-fronts (i.e., gust fronts), meso high/low, unless they are resolved by the initial fields.
- iv) Rather crude specification of surface parameters, such as albedo, emissivity, soil moisture, snow, etc.
- v) Somewhat time-consuming to run at resolutions less than 5 km.
- vi) The present BFM uses only 16 computational layers and extends up to 7,000 m above the highest grid point of model domain, in order to save computational time.

The BFM forecasting capability will be improved when the output of the regional scale forecasting models such as the US Air Force's Relocatable Window Model (RWM) or the US Navy Operational Regional Atmospheric Prediction System (NORAPS) are used instead of the GSM. The GSM output is at present available every 381 km. We will start studying the

utilization of finer grid model output to initialize the BFM.

VI. References

Gelding, B. W., 1990: The meteorological office mesoscale model, *Meteorological Magazine*, 119, 81-96.

Mellor, G. L., "The Gaussian Cloud Model Relation", *Journal of Atmospheric Sciences*, 34, 356-358, 1977.

Pielke, R. A., "Mesoscale Meteorological Modeling", Academic Press, New York, 1984.

Sommeria, G. and J. W. Deardorff, "Subgrid Scale Condensation in Cloud Models", *Journal of Atmospheric Sciences*, 34, 344-355, 1977.

Sundqvist, H., E. Berge and J. E. Kristjánsson, "Condensation and Cloud Parameterization Studies with a Mesoscale Numerical Weather Prediction Model", 117, 1641-1657, 1989.

Yamada, T. and S. Bunker, "A Numerical Model Study of Nocturnal Drainage Flows with Strong Wind and temperature gradients", *Journal of Applied meteorology*, 28, 545-554, 1989.

Yamada, T., and G. L. Mellor, 1979: A simulation of BOMEX data using a turbulence closure model coupled with ensemble cloud relations, *Quarterly Journal of the Royal Meteorological Society*, 105, 915-944.